Theoretical Aspects of Scrap Dissolution in Oxygen Steelmaking Converters

G. Sethi[a], A. K. Shukla[a], P. C. Das[b], P. Chandra[b] and B. Deo[a]
[a]Department of Materials and Metallurgical Engineering,
[b]Department of Mathematics
Indian Institute of Technology Kanpur, 208016
Tel: +91-512-2597256
Fax: +91-512-2597505
Email: {guneet.sethi@alumni., akshuk@, pcdas@, peeyush@, bdeo@} iitk.ac.in

Keywords: BOF, scrap dissolution, analytical, Fourier, finite difference

INTRODUCTION

The scrap dissolution rate in BOF is known to affect the bath temperature, slag formation, foaming of slag and post combustion in the first 8-10 minutes of blow. Kinetics of scrap dissolution essentially belongs to the class of moving boundary problems with phase change (Stefan problems). Although literature is replete with solutions of Stefan problems, a complication in the case of scrap dissolution in BOF is that the bath (liquid metal) temperature and composition change with time. Several models of scrap dissolution in BOF have been published in literature[1-10] and in each model simplifying assumptions have been made.

The mechanism of scrap dissolution comprises of simultaneous heat transfer and mass transfer (of carbon) in the melt and inside the scrap. The process of dissolution can be divided into following three parts:

1. "Solidification" of liquid metal on the parent scrap (chill effect)
2. "Fast melting" of the solidified shell
3. "Normal melting" of the parent scrap

The rate of solidification or dissolution may be defined as the product of scrap-melt interface area and velocity of the interface. The velocity of the scrap-melt interface at any moment depends upon (Figure 1) the thermal conductivity of the scrap, heat transfer coefficient of the melt, temperature difference between interface and the bulk, temperature gradient inside the scrap and at the interface and latent heat of melting. The interface temperature and composition are related to the equilibrium iron-carbon phase diagram.

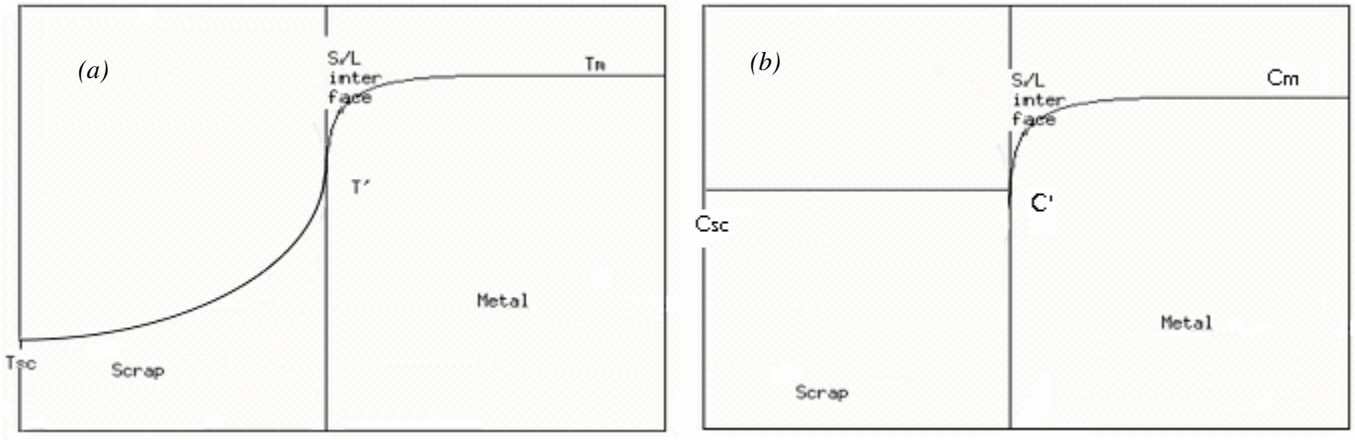

Figure 1: Temperature (a) and carbon concentration (b) profiles in scrap and metal

Among all the investigations reported so far the key items of discussion have been the method estimation of temperature gradient inside the scrap, composition (carbon content of the solidified skin) of scrap and the composition of the liquid melt at the interface during melting. The theoretical basis of some the important investigations are critically examined before proceeding to develop an analytical model.

Hartog et al[1] developed an interesting numerical procedure based on solution of simultaneous, unsteady state, heat transfer and mass (carbon) transfer equations at the bath-scrap interface. They considered moving boundary layer approach to estimate heat transfer coefficient and Chilton-Colburn analogy to estimate mass transfer coefficient. The scrap-melt interface temperature and carbon composition was deduced from Fe-C phase diagram. The rates of energy generation due to chemical reactions were calculated from off-gas analysis and bath sampling. The heat losses from BOF were calculated by posteriori calculations in real heats. Solutions were obtained for different sizes of scrap and carbon content. The evolution of temperature of the bath and complete dissolution of the scrap depended upon the scrap size distribution. In the presence of higher proportion of light scrap, the temperature of the bath was predicted to be almost near to the liquidus temperature. Dissolution of the colder heavy scrap had to wait until the light scrap dissolved. The diffusion of carbon inside the solid scrap was not considered. Szekely[2,3] considered the diffusion of carbon from melt into the solid scrap and assumed that melting process was controlled by mass transfer of carbon from the melt. Specht and Jeschar[4] assumed bath temperature and composition to be constant. The diffusion of the carbon inside the solid scrap was considered by using Ficks' law. Solidification of metal on scrap (chilling effect) was not considered. The temperature profile at the interface was calculated by considering the solid as a semi-infinite body. The heat of fusion included an additional term to account for the energy required to raise the temperature of melting mass from interface temperature to the bulk temperature. The heat and mass transfer coefficients were estimated by Sherwood and Nusselt numbers for spherical, cylindrical and laminar-slab shaped solids under forced convection conditions. The time for complete melting was proportional to the initial size of the scrap. Gaye and Wanin[5] considered heat transfer coefficient as a function of input energy to the system and thus incorporated the effect of blowing conditions on heat and mass transfer coefficients. They also studied (similar to Hartog et al[1]) the dissolution behavior for different thickness and scrap mixes. The permissible limits of scrap size, to ensure complete melting by the time of in-blow sublance measurement, were recommended. As expected, bottom stirring improved the melting rate significantly. Preheating of the heavy scrap did not improve its dissolution rate even if blowing time was increased. Yoruchu and Rolls[6] employed finite difference procedure and considered the diffusion of carbon inside the scrap. Diffusion Coefficient depended upon temperature (given by Arrhenius relationship). They assumed that carbon composition at the scrap surface was same as that of bath and the temperature as equal to the melting point of the bath.

Asai and Muchi[7] presented a detailed model for scrap dissolution in BOF. Temperature and carbon concentration of the melt were considered as important variables and their influence on progress of the melting of the scrap for different operating conditions was investigated. They assumed the temperature and concentration profiles only inside the liquid at the interface. The composition of the solidified shell was assumed to be same as that of the scrap; this is however not true (see discussions later in the paper). Temperature inside the scrap at any moment was considered to be uniform and the velocity of the moving interface was considered to be constant; these approximations are however valid only for the case of thin scraps. Gupta[8,9] considered a uniform temperature and carbon composition inside the scrap but a steep temperature and composition gradient at the interface for a semi-infinite body (similar to Asai and Muchi[7]). The composition of the solidified layer was assumed to follow the changes in bulk liquid metal composition as a function of time. The interfacial velocity was calculated at each time step but was found to be nearly constant during the major period of scrap dissolution (except towards the end of dissolution). The effect of various parameters on the peak value of solid (scrap + solidified shell) to liquid ratio, for a given scrap to hot metal ratio and for different preheat temperatures and heat generation factors, were studied. The amount of build up of solidified shell was predicted to be up to 33% of the initial scrap mass, which is rather high.

Zhang and Oeters[10,11] considered the dissolution of sponge iron and scrap in high carbon melts. For the different stages of solidification, three simultaneous equations involving heat transfer, carbon mass transfer and carbon-temperature relationship (as given by liquidus line) were solved for the three unknowns, namely, carbon and temperature at the interface and the velocity of the moving interface. During frozen shell development, interface carbon content in liquid and solid phases was related to the Fe-C phase diagram. The thermal boundary layer was assumed to form as soon as the scrap came into contact with the liquid whereas the development of concentration boundary layer took some time due to the slow process of mass transfer. It was shown that heat transfer was nearly forty times faster than mass transfer during the initial period of shell formation. Since the initial solidification velocity was high due to the steep temperature gradient, the initial frozen layer had the same composition as that of the melt (decided by Fe-C phase diagram). As the velocity of the shell formation reduced the concentration boundary layer was established at the interface. The time beyond which contribution of thermal gradient inside the scrap could be neglected was calculated.

According to some of the earlier investigations[12], the contribution of frozen layer to overall melting process can be ignored. For example, Goldfarb and Sherstov showed that the total time for solidification and fast melting is less than 2 minutes in the case of a sphere of 20 cm diameter iron rod, for a heat transfer coefficient of 24000 J/m^{2}s. According to Phelke also, the freezing causes delay of only 30 seconds for melting of bar of 3.7 cm in diameter. Fatukami et al reported that a 15 cm thick flat plate scrap melts between 16 to 20 minutes. Hills concluded that the melting rate was very sensitive to the temperature-carbon-time profile and the most important aspect of the blowing path in BOF is to develop a difference as large as possible, at any temperature, between the carbon content of the bath and liquidus of the Fe-C system. Thus, by creating optimum conditions inside the BOF, it may be possible to melt even very thick ingots (71 cm thick) in as little time as 23 minutes; Hills assumed the mass transfer coefficient of the order of 2.5 x 10^{-4} m/s and heat transfer coefficient of the order of 20000 J/m^2 s.

In the actual BOF process even the heat transfer coefficient varies with time due to changes in fluid flow conditions imposed by the impinging oxygen jet as well as scrap geometry due to presence of a mixture of heavy scrap and light scrap of various sizes. In fact it is not possible to simulate the conditions of scrap dissolution in BOF under laboratory conditions. In the present work theoretical aspects of scrap dissolution are discussed and, for the first time, an analytical model is developed so as to verify the results of finite difference models or numerical models which have been normally employed so far.

MODEL DESCRIPTION

Analytical Model

The basic assumptions made in the analytical model are:

1. No mass transfer control during the solidification and fast melting stage.
2. Convective heat transfer in the melt.
3. $v = \dfrac{\Delta L}{\Delta t}$ is constant in the small time step, Δt . This velocity would be positive in the initial solidification and would be negative in the subsequent stages.
4. $\dfrac{dW_m}{dt} = -\dfrac{dW_{sc}}{dt} - \sigma_1 s$ where $\dfrac{dW_{sc}}{dt} = \rho A v$. The amount of carbon consumed by the CO reaction is also included in the weight balance.
5. Since specific heat of scrap would be varying with temperature we would find out its average value using the interface temperature and center line temperature of scrap. The temperature dependence is as follows:

$$C_p^{sc}(T) = 17.49 + 24.769\times10^{-3}T \quad \textit{(J/molK)}$$

Attention will be given to the ratio of solid metal to liquid metal in the early stages of the blow in converter as a function of hot metal temperature, rate of heat generation due to oxidation reactions, scrap to hot metal ratio in the charge, as well as the actions taken during the blow (change of lance height and amount and timing of coolant additions).). Effect of heat transfer coefficient on kinetics of scrap dissolution and the solid to liquid ratio will be examined.

Governing Equations

From figure 1, following equations are formulated:

1. Heat Flux Balance at the interface x=0:

$$hA(T_m - T') = \rho A(-\Delta H_{Fe})v - \lambda A\left.\frac{\partial T_{sc}(x,t)}{\partial x}\right|_{x=0} \tag{1}$$

Here $\lambda = \rho C_p^{sc}\alpha$ where C_p^{sc} is the average specific heat for the scrap calculated using one end temperature as the interface temperature (T') and the other as the center line temperature is T_{sc}.

The term ΔH_{Fe} will have contributions depending on the stage of process:

- Solidification: The term ΔH_{Fe} incorporates heat of fusion as well as the heat required to raise the temperature of liquid metal from interface temperature (T') to the temperature of melt (T_m).

$$\Delta H_{Fe} = \Delta h + c_p (T_m - T') \quad (2)$$

- Fast Melting: The term ΔH_{Fe} incorporates heat of fusion as well as the heat required to raise the temperature of scrap layer (T_{av}) to the temperature of melt(T_m).

$$\Delta H_{Fe} = \Delta h + C_p (T_m - T_{av}) \quad (3)$$

T_{av} is calculated as: $$T_{av} = \frac{\int_0^{\Delta L} T_{sc}(x,t)\partial x}{\Delta L} \quad (4)$$

- Normal Melting: Similar to fast melting the term ΔH_{Fe} incorporates heat of fusion as well as the heat required to raise the temperature of scrap layer (T_{av}) to the temperature of melt(T_m).

$$\Delta H_{Fe} = \Delta h + C_p^{sc1}(T' - T_{av}) + C_p^{sc2}(T_m - T') \quad (5)$$

C_p^{sc1} is the average specific heat for the scrap at temperature T_{av}. C_p^{sc2} is the average specific heat for the scrap calculated using one end temperature as the interface temperature (T') and the other as the melt temperature T_m. T_{av} is again calculated as in (4)

To solve the heat balance heat equation (1) we need to know the temperature distribution of the scrap, $T_{sc}(x, t)$. For one dimensional heat flow, the Fourier Equation states

$$\alpha \frac{\partial^2 T_{sc}(x,t)}{\partial x^2} = \frac{\partial T_{sc}(x,t)}{\partial t} \quad (6)$$

Solving equation (6) (available in Appendix I) we obtain the following solution:

$$T_{sc}(x,t) = T' + \sum_{n=1}^{\infty} A_n \sin\frac{n\pi x}{2L} \exp(-\lambda^2 \alpha t) \quad (7)$$

The limitation of this solution is the fixed boundary temperature and constant dimension which in our case are changing with the time. Hence we devise a step wise solution procedure in which the whole run time is divided into several time steps (Δt). The initial form of solution for any time $t=m\,\Delta t$ and $t_{prev}= (m-1)\,\Delta t$ as seen from (7) and by calculating A_n, is:

$$T_{sc}(x, m\Delta t) = T' + \sum_{n=1}^{\infty} \frac{(1-\cos n\pi)}{\frac{n\pi}{2}} (T_{sc}^{i} - T') \sin\frac{n\pi x}{2L} \exp(-\lambda^2 \alpha (m\Delta t)) \quad (8)$$

where T' and L are values used from previous time step, $(m-1)\Delta t$.

Hence using (7) or (8) we get $$\left.\frac{\partial T_{sc}(x,t)}{\partial x}\right|_{x=0} = \sum_{n=1}^{\infty} A_n . \frac{n\pi}{2L} \exp(-\lambda^2 \alpha t) \quad (9)$$

where A_n can be evaluated from Appendix I.

Once $T_{sc}(x,t)$ is known, then T_{av}, v can be obtained from (7). Thus

$$T_{av} = \frac{2L}{\Delta L}\left\{\sum_{n=1}^{\infty}\frac{A_n}{n\pi}(1-\cos\frac{n\pi\Delta L}{2L}).\exp(-\lambda^2\alpha t)\right\} \tag{10}$$

$$v = \frac{1}{\rho(-\Delta H_{Fe})}\left\{h(T_m - T') + \lambda\left.\frac{\partial T_{sc}(x,t)}{\partial x}\right|_{x=0}\right\} \tag{11}$$

Thus we can solve for the melting velocity at each time step from (11).

2. Mass transfer control in liquid metal:
   - Solidification: $C' = C_m$ (12)
   - Fast Melting: No mass transfer control in liquid metal

     $$C' = f(W_{sc}) \tag{13}$$

     The different portions of skin have different carbon concentration and that is equal to carbon concentration in melt during the skin formation stage. So we can take C_m values with respect to thickness in solidification stage and regress the data for polynomial regression. Due to lesser accuracy of the regressed constants, this caused jump of the carbon concentrations at the interface and melt at the start of Normal melting stage. We ignore such a jump as it doesn't cause an occurrence of error in the calculations.
   - Normal Melting: No Mass transfer control in liquid metal

     $$C' = C_m \tag{14}$$

     Mass transfer can be considered to be rate controlling if the following equation is followed:

     $$k(C_m - C') = v(C' - C_{sc}) \tag{15}$$

3. Phase Diagram Equation: The following equation is used for solidus line

   $$T' = 1809 - 90C' \tag{16}$$

4. Change in heat content of melt:

   - Solidification: $C_p\frac{d(W_m T_m)}{dt} = \Delta H_{co}\sigma_1 s - hA(T_m - T') + C_p T_m\frac{dW_m}{dt}$ which on simplification

     yields $C_p W_m\frac{dT_m}{dt} = \Delta H_{co}\sigma_1 s - hA(T_m - T')$ (17)

   - Fast and Normal Melting: $C_p\frac{d(W_m T_m)}{dt} = \Delta H_{co}\sigma_1 s - hA(T_m - T') - C_p T_{av}\frac{dW_{sc}}{dt}$ which

     on simplification yields:

$$C_p W_m \frac{dT_m}{dt} = \Delta H_{co}\sigma_1 s - hA(T_m - T') + C_p((T_m - T_{av})\frac{dW_{sc}}{dt} + T_m\sigma_1 s) \quad (18)$$

5. Change in carbon content of melt:

- Solidification: $\frac{d(W_m C_m)}{dt} = -\sigma_1 s - \beta C_m \frac{dW_m}{dt}$ which on simplification yields

$$W_m \frac{dC_m}{dt} = -\sigma_1 s - C_m(\beta + 1)\frac{dW_m}{dt} \quad (19)$$

- Fast Melting: $\frac{d(W_m C_m)}{dt} = -\sigma_1 s - C_s \frac{dW_{sc}}{dt}$ On simplifying we get:

$$W_m \frac{dC_m}{dt} = -\sigma_1 s + ((C_m - C_s)\frac{dW_{sc}}{dt} + C_m\sigma_1 s) \quad (20)$$

where $C_s = C'$ at that instant of time.

- Normal Melting: $C_s = C_{sc}$ in (20) (21)

The scheme of calculation sequence is explained in Figure 2.

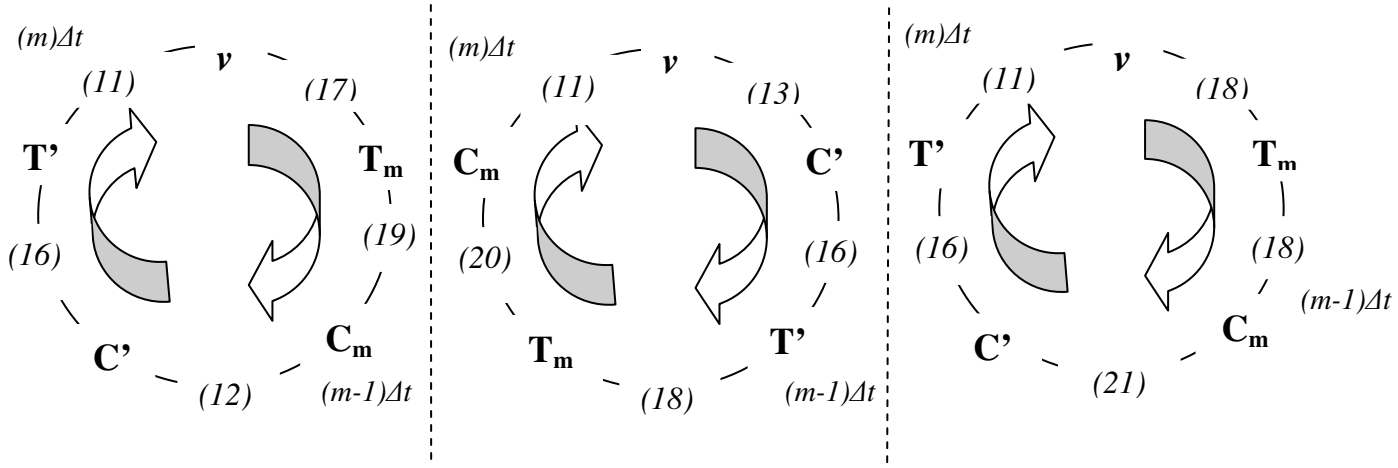

(a) (b) (c)

Figure 2: Calculation sequence in the simulation used for solving the solidification stage (a) fast melting stage (b) and normal melting stage (c)

The solidification stage will continue till $\frac{dW_{sc}}{dt} \geq 0$ corresponding to the maximum thickness of the solidified layer.

The fast melting stage will continue till W_{sc} returns to its initial value when the experiment was started, corresponding to removal of the solidified layer. The normal melting stage will continue till whole of the scrap piece melts.

Numerical model

We would like to compare the results of the numerical finite difference method (FDM) only in the normal melting stage. Hence we would be given the temperature distribution and other such variable values after the solidification and prior to melting are taken from the analytical solution. The details of the FDM procedure are provided elsewhere[8]. More details on the formulation are also available[9,15].

RESULTS AND DISCUSSION

Mass Transfer vs. Heat Transfer

Mass Transfer can be considered to be rate controlling if the following equation is followed:

$$k(C_m - C') = v(C' - C_{sc}) \tag{15}$$

We note that at the end of the melting stage the k^{ξ} and v are in comparison and hence we will be able to find out the value of C_m (which would be near to the value of C_{sc}) such that mass transfer is rate controlling. Thus it is noted that during the initial period of normal melting heat transfer is rate controlling while in the later end stages when the carbon concentration has decreased to a large extent then mass transfer is rate controlling. By the analyzing the sensitivity of the interface temperature with the mass transfer co-efficient we are able to arrive at and appropriate value of mass transfer co-efficient such that our model works in conjunction with what is expected (total melting time observed in the actual process), when we assume the process to be heat transfer controlled. We were able to find out value of such a mass transfer co-efficient that after attaining that value the mass transfer becomes asymptotic to heat transfer. The value amounts to .005 m/s as seen in Figure 3. It can be seen that the condition of mass transfer coefficient of 0.005 m/s corresponds to a particular fluid flow situation in BOF. In actual practice the mass transfer coefficient will change with time, depending upon the operating conditions of bath mixing oxygen flow, lance height, scrap mixture of different sizes, etc.). Our aim here is to demonstrate the application of analytical method and compare it with the numerical solution for the same set of initial and boundary conditions.

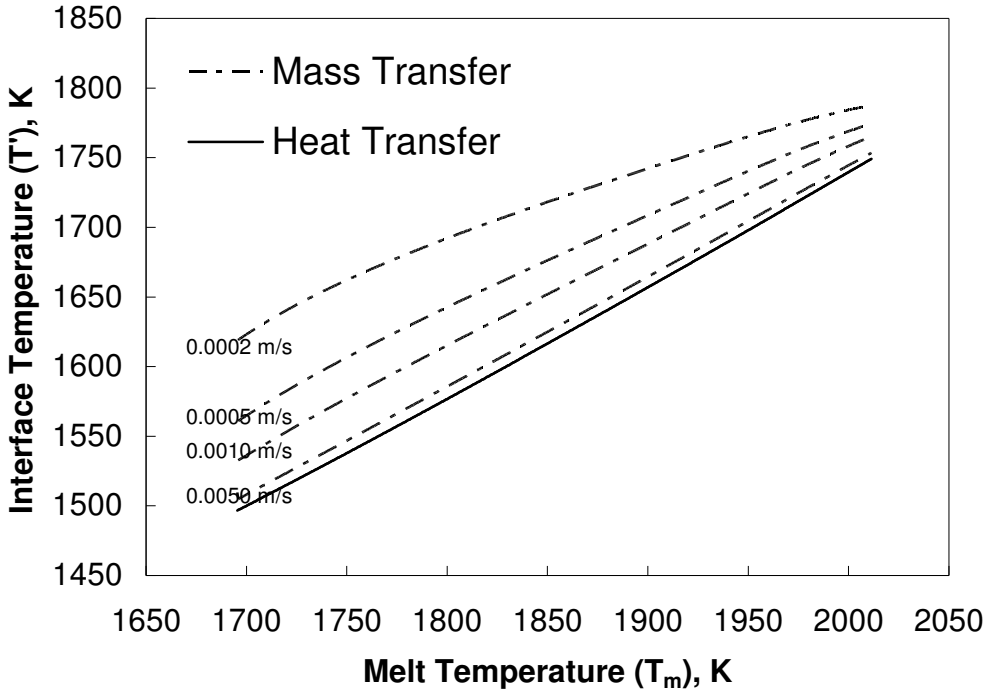

Figure 3: Variable mass transfer and heat transfer

[ξ] Value from literature

Fourier Series Solution vs. Finite Difference Solution

Figure 4 compares the variation of the each of the parameters in the Fourier solution (which is the analytical solution) and the finite difference solution (which is the numerical solution).
Figure 4(a) showing the length of the scrap, clearly depicts the occurrence of stepped profile in finite difference method. This was expected since FDM is a numerical procedure. Both analytical and FDM have similar average profiles although incomplete melting is observed in the analytical method. This occurs due to non-equilibrium nature of the present analytical solution. This is one of the drawbacks of the analytical methods in the sense that the scrap gets melted at a sharp temperature whereas in the actual case there would be a melting range as would be seen in the results of the finite difference method. Thus in the analytical solution complete scrap would melt only if the temperature of the scrap is equal to the melting point. Since length and weight are proportional Figure 4(h) shows a similar trend.

Figure 4(b) shows that at the end of the cycle the melt velocity, *v* reached is 0.00035m/s. The melt velocity doesn't remain constant but instead decreases, although the decrements are gradual. Thus we see that the interface movement velocity is not constant as assumed by Asai and Muchi[7].

Figure 4(c) and 4(d) demonstrate the variation of interface temperature (T') and melt temperature (T_m). The temperature rise is slightly lower in FDM, which implies that more heat is extracted by the scrap in the FDM. This could possibly be attributed to the existence of a large mushy range. To justify such a large melting range we say that the heat flow is much easier in FDM compared to the Fourier solution where there is heat concentration. Thus this forced rising of the temperature caused the melting rate to be higher and the heat flow as such through conduction into the material is low which leads to formation of a steep profile. No such artificial rise was used in the case of analytical solution and hence the profile was consistent with the expected (a parabolic profile) which clearly depicts the power of an analytical solution and weakness of numerical solution.

Figure 4(e) and 4(f) demonstrate the variation of interface carbon concentration (C') and melt carbon concentration (C_m). The melt carbon concentration is slightly higher in the finite difference solution which implies that the chances of FDM to be driven by mass transfer control are less.

Figure 4(g) shows the variation of centre line temperature of scrap. A steep rise is observed in the case of FDM as opposed to a steady rise in the case of analytical solution. This could be explained on the basis of mass transfer occurring in the system. The FDM solution doesn't scope in possibility of mass transfer. In the end the process will become mass transfer controlled rather than heat transfer controlled. Thus the temperature rise should not be as steep as observed in the FDM solution. Hence the analytical solution depicts the correct nature of the process. Also, the heat extraction is by the scrap is more in FDM (Figure 4(c)) and yet the temperature rise of the scrap is smaller. This is because of the existence of such a large mushy range. Another thing to note is that the temperature at all points at all times is higher in analytical solution than in the case of numerical solution.

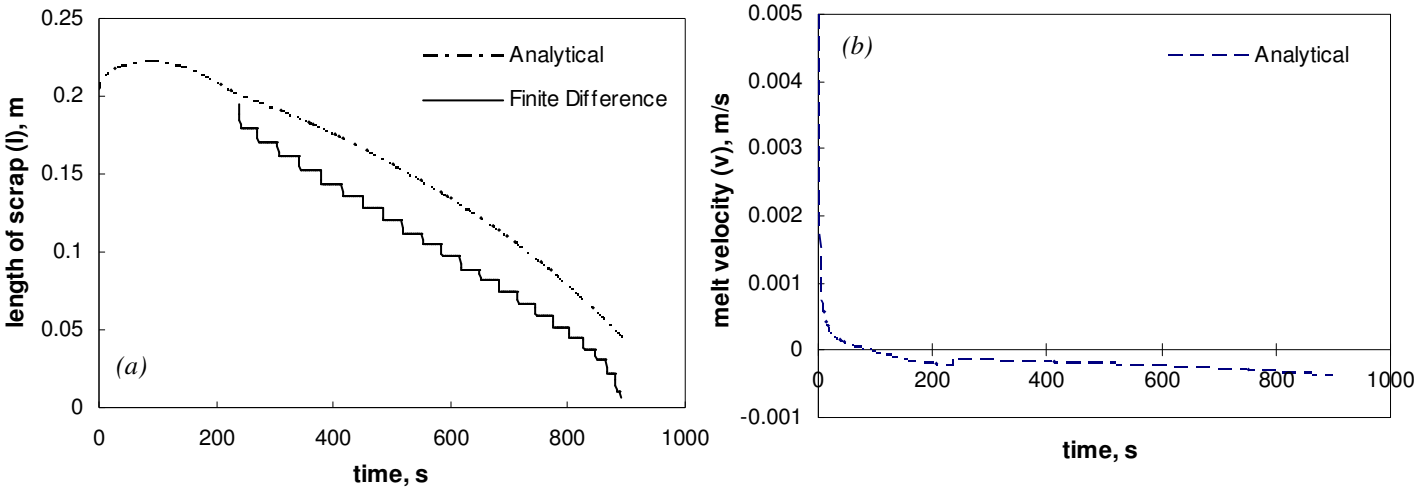

Figure 4(i) and 4(j) show the temperature profiles in the analytical solution and the finite difference solution. The profile is steep in FDM in comparison with Fourier solution which has a near parabolic profile.

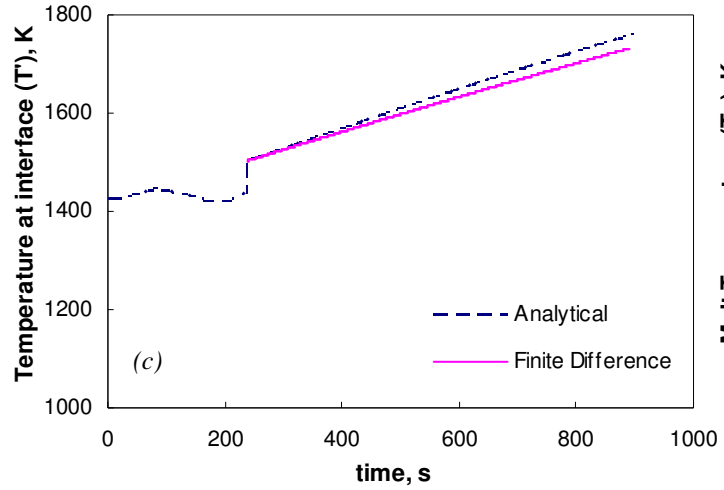

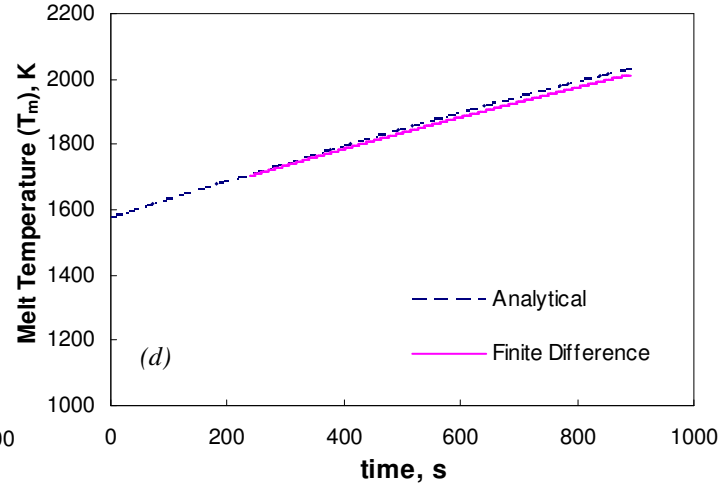

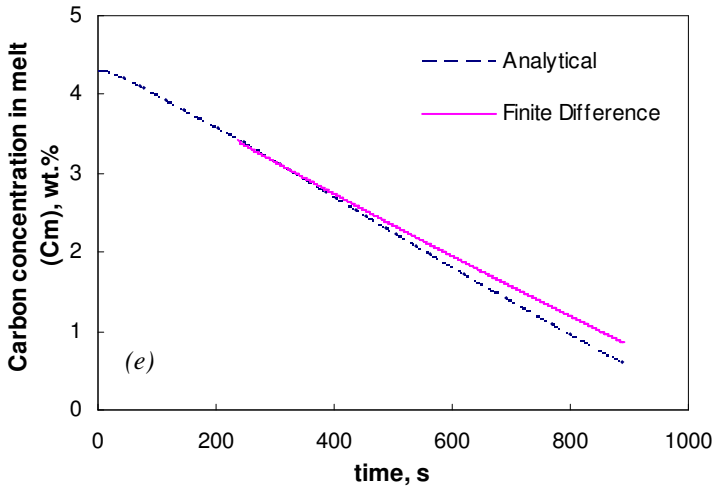

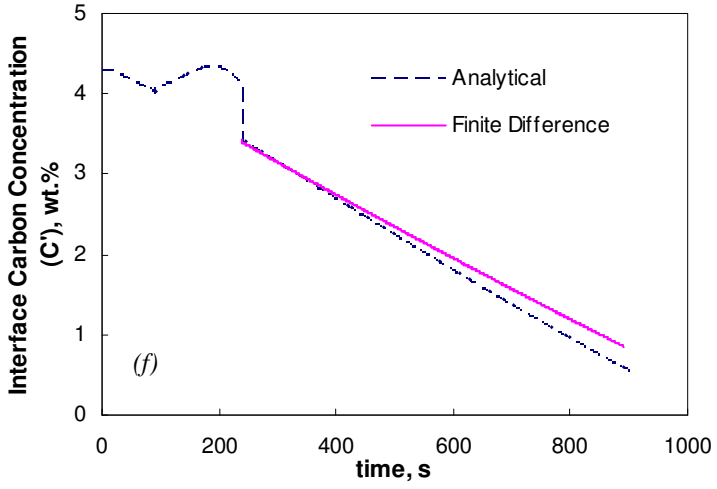

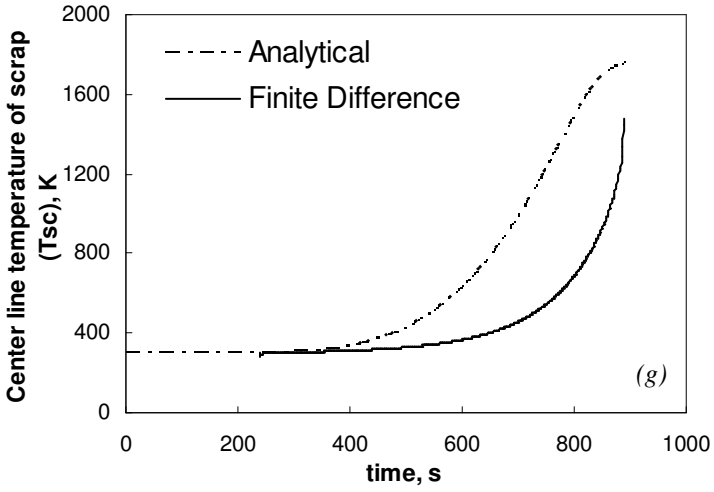

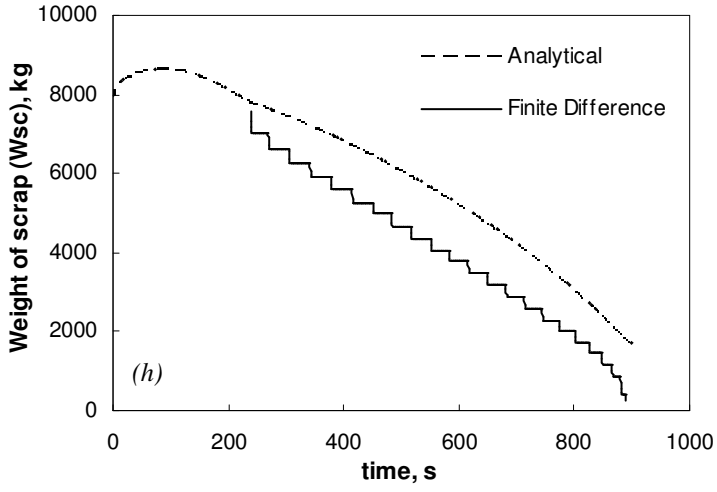

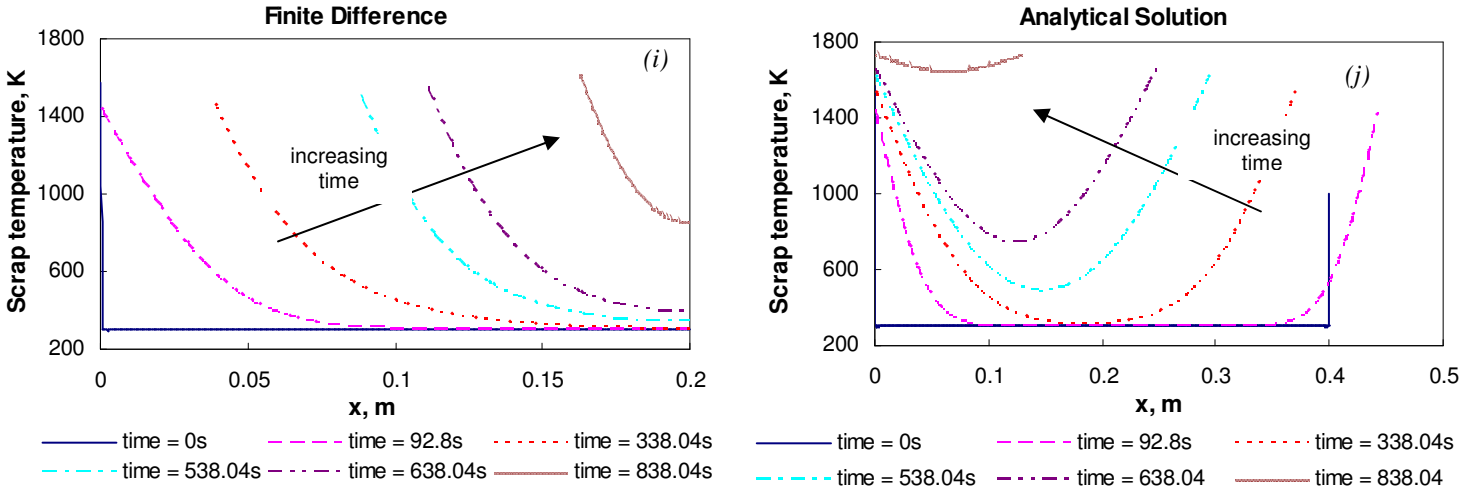

Figure 4: Variation of different parameters with time in finite difference solution and analytical solution

Effect of Heat Transfer Co-efficient

As heat transfer into the scrap will increase the melting rate will increase. The higher heat transfer into the scrap will cause a drop in the temperature of melt as seen in the case of 10 times 'h' in figure 5(a). This drop was also observed in the experimental data by Specht and Jeschar[4]. The drop of melt temperature negates the effect of higher melting rate thus restoring the solution towards an equilibrium solution. Overall, the incomplete melting decreases (Figure 5(b)). Also the solidified shell thickness and time decreases which was expected due to steeper rise in the overall temperature of the scrap.

Recent laboratory experiments have shown that when an iron rod is dipped into carbon saturated molten iron at 1673 K then the frozen (chilled) shell formed on the iron rod is not in perfect contact with the parent iron rod; the SEM shows a very thin but not totally uniform gap between the iron rod and the frozen shell. This phenomenon will affect the heat transfer between the frozen shell and the parent iron rod in an undetermined way. For this reason we have compared the results of analytical model with the FDM model only after the melting of the frozen layer, with an assumed temperature profile in the scrap. Further experiments are in progress to characterize the formation of frozen shell so as to see the variation of carbon content along the thickness of the shell.

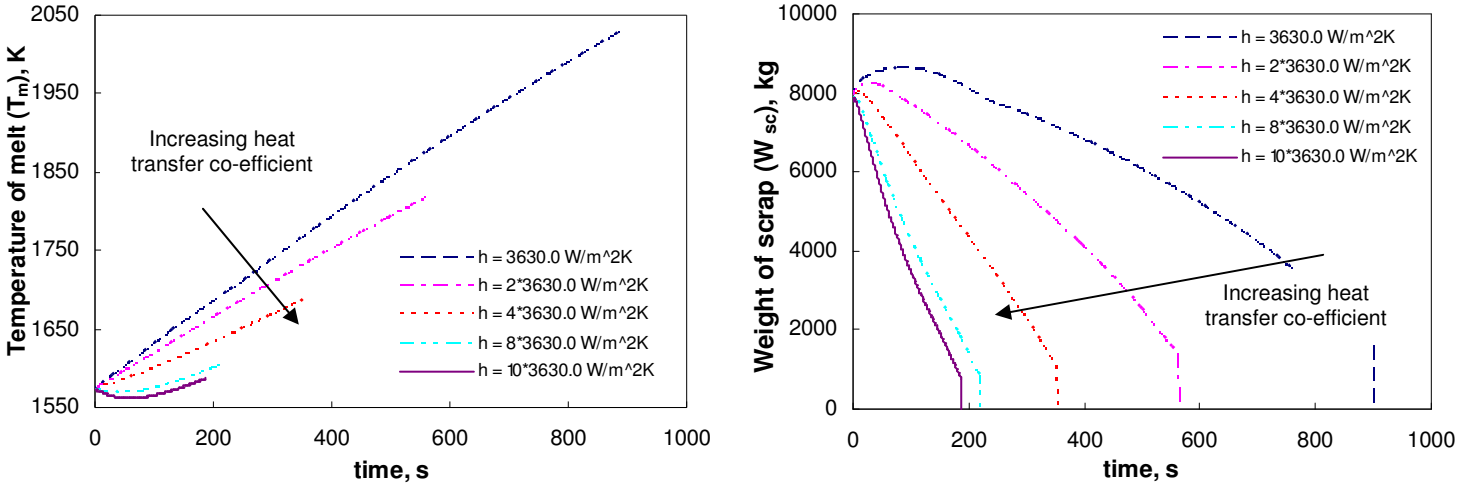

(a) (b)

Figure 5: Effect of heat transfer co-efficient

SUMMARY

A new model based on analytical solution of heat and mass transfer equations using a Fourier series based solution of the temperature distribution in the scrap is described. The results are critically compared with the FDM solution. The velocity of the solid-liquid interface movement is evaluated at each time step. The temperature profile predicted by analytical solution is likely to be more accurate than the FDM solution because of the assumption of mushy zone in the latter. The difference in temperature profile between analytical solution and FDM solution is clearly reflected in the manner of rise of center line temperature. Further experimental work is, however, needed to study the thermal consequences of lack of perfect thermal contact between the solidified (chilled) layer and the core solid metal (scrap).

REFERENCES

1. H.W. Hartog, P.J. Kreyger and A.B. Snoeijer, *C.R.M,* No.37, December 1973 pp.13-21
2. J. Szekely, Y.K. Chuang and J.W. Hlinka, "The melting and dissolution of low carbon iron-carbon melts", *Metallurgical Transactions*, 3, 1972, pp. 2825-2833
3. Y.K. Chuang and J. Szekely, *International Journal of Heat and Mass Transfer*, 14, 1971, pp.1285-1294
4. E. Specht and R. Jeschar, *Steel research*, 64, 1993, pp. 28-34
5. H. Gaye, J. Wanin, P. Gugliermina and P Schittly, *Proc. 68th Steelmaking Conference, Detroit, U.S.A,* April 14-17, 1985, pp.91-102
6. H. Yoruchu and R. Rolls, *Iron and Steel International*, February 1976, pp.35-39
7. S. Asai and I. Muchi, *Transactions ISIJ*, 11, 1971, pp.107-115
8. Brahma Deo, Gaurav Gupta and Manish Gupta, *Proc. Asia Steel Int. Conf. Jamshedpur India, April 9-12*, Vol. 02, 2003, pp. 2.d.1.1-2.d.1.8
9. G.K. Gupta, *B.Tech Report*, Department of Materials and Metallurgical Engineering, I I T Kanpur, 1998
10. Liuyi Zhang and Franz Oeters, "Melting and mixing of alloying agents in steel melts", *Verlag Stahleisen Gmbh, Dusseldorf*, 1999, pp.87-91
11. Liuyi Zhang and Franz Oeters, *Steel Research*, 71, No. 5, 2000, pp. 141-144
12. R.D. Phelke, W.F. Porter, R.F. Urban and J.M. Gains, *BOF Steelmaking*, Vol. 02, pp. 219-234
13. E. Kreyszig, *Advanced Engineering Mathematics*, Wiley John & Sons, Incorporated 7th Edition, August 1992
14. J. Szekely, *Process optimization, with applications in metallurgy and chemical engineering*, Wiley, New York, 1973
15. J.P. Holman, *Heat transfer*, 9th ed., McGraw-Hill, New York, 2002

NOMENCLATURE

Notation	Description	Typical values	Units
A	Area of solid/liquid interface	5.4	m^2
C_p	Specific heat of melt	-	J/kgK
C_p^{sc}	Average Specific heat of scrap	0.01	J/kgK
C_m	Bath (Liquid Melt) carbon concentration	4.26	wt. % C
C′	Carbon concentration of S/L interface (liquid)	-	Wt. % C
h	Heat transfer coefficient in liquid metal	3.63*1000	W/m^2K
k	Mass transfer coefficient	.0002	m/s
T′	Temperature of Solid/liquid interface	-	^oK
T_m	Temperature of liquid metal	1573	^oK
T_{sc}^i	Initial temperature of the scrap at the start of experiment	303	^oK
T_{sc}	Center line temperature of scrap	-	^oK
W_m	Mass of melt	38880	kg
W_{sc}	Mass of scrap	.2*38880	kg
ρ	Density of scrap	7200	kg/m^3
λ	Thermal conductivity of scrap	-	W/m^oK
ΔH_{CO}	Enthalpy change in decarburization	(-33000.0*4.2)/12.0	kJ/kg of

			carbon
ΔH_{Fe}	Enthalpy change in scrap melting and raising the temperature of liquid metal to interface temperature	66.0*4.2	kJ/kg Fe
Δh	Enthalpy change in melting of scrap	-	kJ/kg Fe
α	Thermal diffusivity of scrap	.0000062	
L	Half of the total thickness of scrap		M
σ_{1s}	Decarburization rate	.13601*12.0	kgs of C/s
β	Distribution co-efficient of Carbon in Liquid and Solid	.2	-
C_s	Carbon concentration of solidified scrap	-	wt. % C
Δt	Time step	0.01	s

APPENDIX I

Solution of Heat equation:

The Fourier Equation states $\alpha \frac{\partial^2 T_{sc}(x,t)}{\partial x^2} = \frac{\partial T_{sc}(x,t)}{\partial t}$ (A1)

Taking $\theta = T_{sc} - T'$ (A2)

We solve equation $\alpha \frac{\partial^2 \theta(x,t)}{\partial x^2} = \frac{\partial \theta(x,t)}{\partial t}$ by separation of variables method

Assuming solution to be of the form $\theta(x,t)=G(x).H(t)$ (A3)

Putting (A3) in (A2) we get => $G''(x) + \lambda^2 G(x) = 0$ and $\dot{H}(t) + \alpha\lambda^2 H(t) = 0$ (A4a & A4b)

The standard solution of (A4a) is of the form:

$G(x) = A\cos\lambda x + B\sin\lambda x$ (A5)

Now applying Boundary Conditions $\theta(0,t) = 0$ and $\theta(2L,t) = 0$ to (A5) (A6a & A6b)

we get $A=0$ and $\lambda = \frac{n\pi}{2L}$ (A7)

$$\Rightarrow\ G_n(x) = B_n \sin\frac{n\pi x}{2L} \quad \text{(A8)}$$

Similarly the standard solution of (A4b) is of the form

$$H_n(t) = C_n \exp(-\lambda^2 \alpha t) \quad \text{(A9)}$$

where λ is calculated from (A7). Combining both the solutions (A8) and (A9) we get

$$\theta_n(x,t) = G_n(x).H_n(t) = A_n \sin\frac{n\pi x}{2L}\exp(-\lambda^2\alpha t) \quad \text{(A10)}$$

$$\text{where } A_n = \frac{1}{L}\int_0^{2L} \theta(x,0).\sin\frac{n\pi x}{2L}.dx$$

which gives the expression for the temperature distribution in a series form as given below:

$$\theta(x,t) = \sum_{n=1}^{\infty}\theta_n(x,t) = \sum_{n=1}^{\infty} A_n \sin\frac{n\pi x}{2L}\exp(-\lambda^2\alpha t) \quad \text{(A11)}$$

or

$$\text{Thus } T_{sc}(x,t) = T' + \sum_{n=1}^{\infty} A_n \sin\frac{n\pi x}{2L}\exp(-\lambda^2\alpha t) \quad \text{(A12)}$$

This is the analytical solution of the Heat Equation. This solution would be later seen as a parabolic profile in the scrap as expected.